Why it is difficult to reconstruct water year discharge at HEMO: Many small sub-basin contributions have to be considered

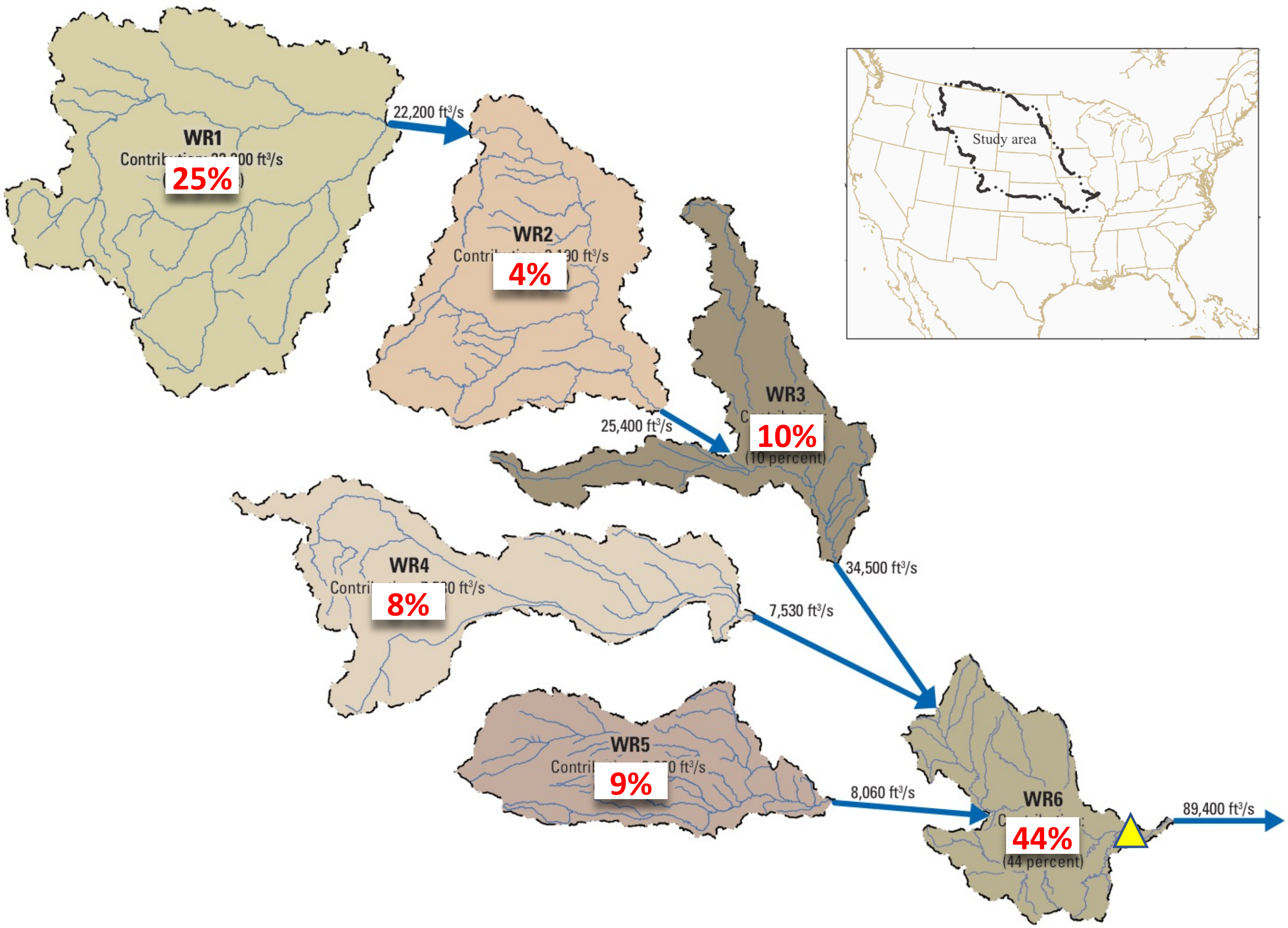

Figure S1. Missouri River watershed regions **WR1-6** contributions to total water year discharge at Hermann, Missouri (△), years 1960-2011. Map modified from Norton et al. (2014, their Figure 16).

Many tree-ring chronologies are available, but not all will be useful. Screening is required: 95% 1-tailed positive correlation used.

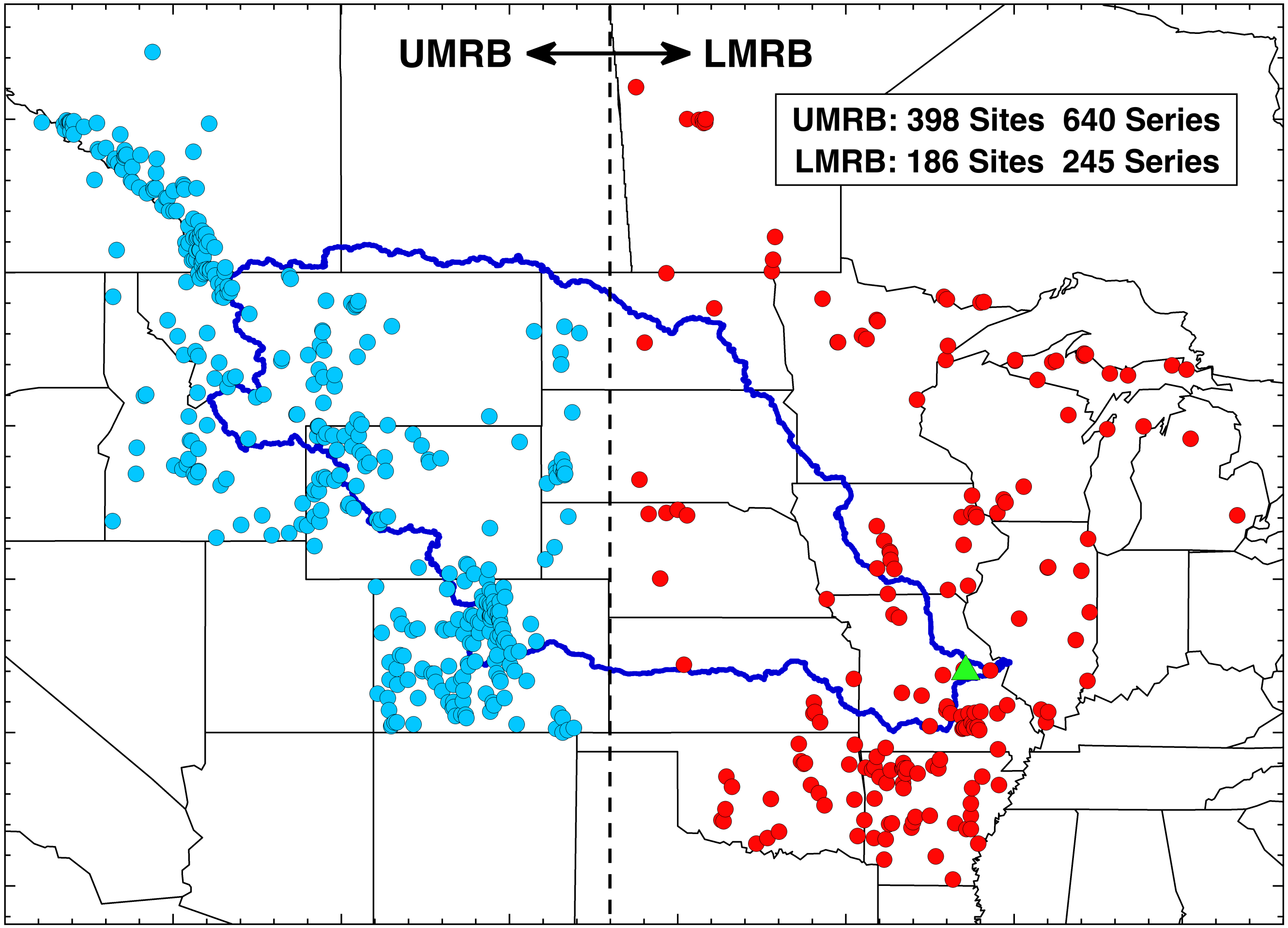

Figure S2. The candidate tree-ring network (896 chronologies) used to reconstruct water year streamflow at HEMO. The network is divided into approximate upper (UMRB) and lower (LMRB) basin sub-networks for screening to a much smaller subset of 'common' tree-ring predictors.

What is the best target streamflow series to use for calibration/validation? McCabe WBM estimates are longer and appear to do an excellent job. ACE appears to have underestimation bias in it as well.

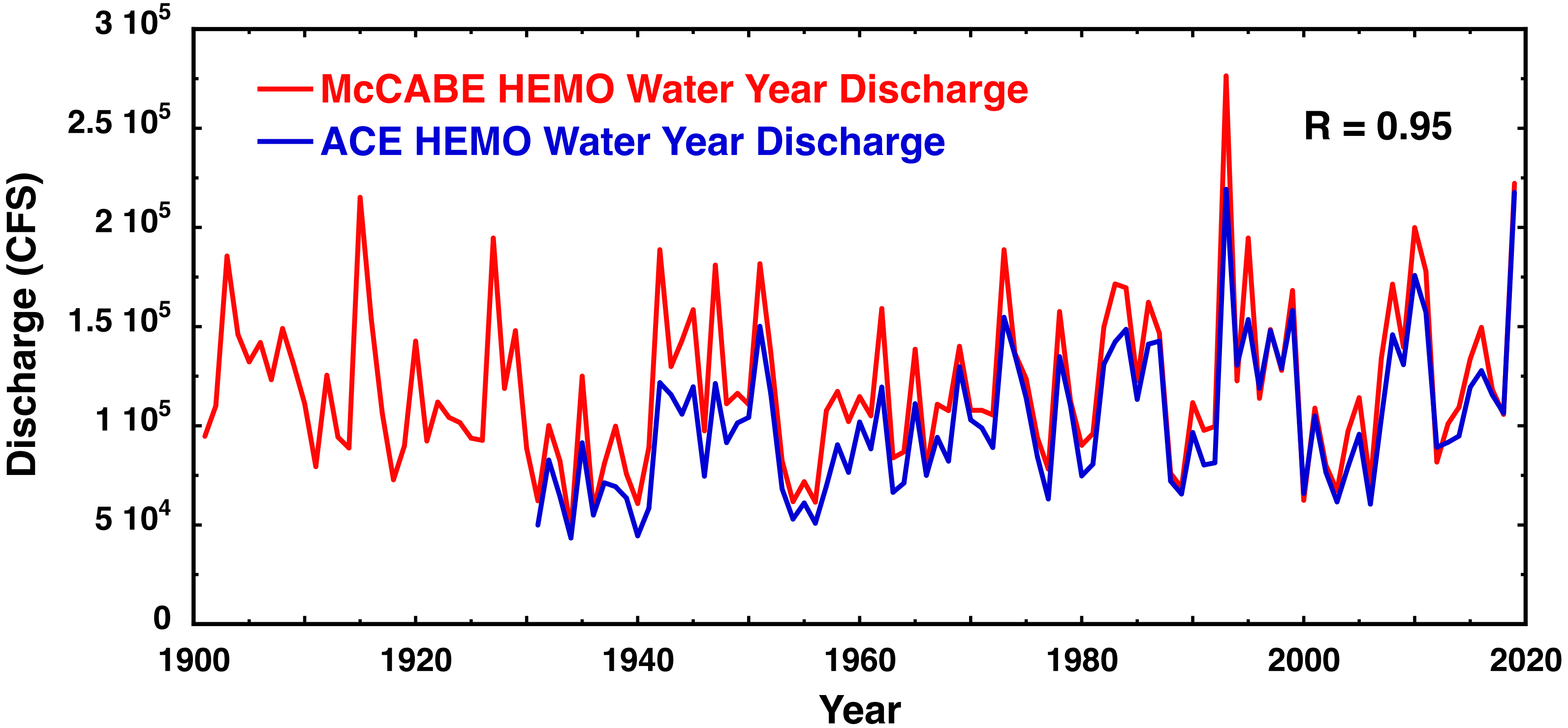

Figure S3. ACE water year discharge estimates at HEMO compared to estimates based on the McCabe water balance model (WBM). This comparison shows that the WBM estimates are sufficiently accurate compared to ACE to be used as the target time series and it also goes back farther to 1901.

Method of Reconstruction:
Principal Component Regression (PCREG)

- ***PCREG*** is a dimension-reducing regression method based on applying principal component analysis (***PCA***) to the suite of ***M*** predictors over the ***N*** year calibration to produce a reduced set of orthogonal predictors that contain most of the useful information in the predictor data set. ***PCA*** is based on the ***correlation matrix*** here to give each predictor equal weight. See Cook et al. (1999, Appendix A) for details.

- Besides dimension reducing, ***PCA*** deals efficiently with ***multi-collinearity*** among the predictors that is frequently encountered when selecting a subset of tree-ring predictors used to reconstruct the same variable.

- ***PCA*** transforms the intercorrelated set of predictors into a new set of orthogonal predictors containing a decreasing level of common signal in their respective principal components (***PC***s) as measured by their eigenvalues. These common signals are loaded most highly the first ***M'*** leading ***PC***s, where ***M'<M***, but only a subset of ***m'*** predictors may be entered into the regression model. ***M'*** is chosen using the Kaiser-Guttman ***Eigenvalue-1 cutoff*** rule. This is the ***'dimension-reducing'*** aspect of ***PCREG***.

- The orthogonality of the ***m'*** predictors entered into the model serves to stabilize the regression model by eliminating ***multi-collinearity***. The entry of variables in the model is also simplified by ordering the variables for testing based on their simple correlations with the predictand variable. The stopping rule for entering variables might be based on the ***minimum AIC*** or ***t-test***. Here a ***t=1.0*** stopping test was used.

Table S1. Tests to determine the most robust set of tree-ring predictors for reconstructing HEMO streamflow. Out of an initial set of 885 candidate predictors (Fig. S2) screened for correlation with HEMO streamflow (95% 1-tailed positive), only 183 were found to have stable correlations with HEMO discharge over two independent calibration periods. Use of these 183 "common" predictors resulted in improved validation statistics in all cases.

Table S1. Tests to determine the most robust set of “common” tree-ring predictors for reconstructing water year discharge for the Missouri River Basin at the HEMO gage (6934500) located at Hermann, Missouri. This determination was made by testing tree-ring chronologies in the Upper and Lower Basins (see Fig. S1) separately for correlation with water year discharge over two equal length calibration periods (1901-1940 and 1941-1980). Only those chronologies that were significantly correlated with HEMO discharge in exceedance of the 95% 1-tailed positive significance level were retained for calibration. The tree-ring chronologies that passed this screening in both calibration periods were then retained as “common” predictors, i.e. those with proven more stable relationships with discharge at HEMO over time. The validation statistics based on these “common” predictors also improved noticeably compared to those not based on this second level of tree-ring predictor screening, thus supporting its use here.

LOWER MISSOURI RIVER BASIN – ALL 95% 2-TAILED SCREENED CHRONOLOGIES							
CALIBRATION	NSER	CRSQ	CVRE	VALIDATION	VRSQ	VRE	VCE
1901-1940	173	0.666	0.638	1941-1980	0.504	0.514	0.487
1941-1980	116	0.696	0.663	1901-1940	0.678	0.676	0.662
LOWER MISSOURI RIVER BASIN – COMMON 95% 2-TAILED SCREENED CHRONOLOGIES							
CALIBRATION	NSER	CRSQ	CVRE	VALIDATION	VRSQ	VRE	VCE
1901-1940	107	0.653	0.624	1941-1980	0.639	0.641	0.621
1941-1980	107	0.700	0.667	1901-1940	0.679	0.672	0.658
UPPER MISSOURI RIVER BASIN – ALL 95% 2-TAILED SCREENED CHRONOLOGIES							
CALIBRATION	NSER	CRSQ	CVRE	VALIDATION	VRSQ	VRE	VCE
1901-1940	180	0.625	0.590	1941-1980	0.260	0.220	0.178
1941-1980	186	0.458	0.391	1901-1940	0.385	0.333	0.306
UPPER MISSOURI RIVER BASIN – COMMON 95% 2-TAILED SCREENED CHRONOLOGIES							
CALIBRATION	NSER	CRSQ	CVRE	VALIDATION	VRSQ	VRE	VCE
1901-1940	76	0.633	0.599	1941-1980	0.353	0.305	0.267
1941-1980	76	0.220	0.139	1901-1940	0.633	0.581	0.564
FULL MISSOURI RIVER BASIN – ALL 95% 2-TAILED SCREENED CHRONOLOGIES							
CALIBRATION	NSER	CRSQ	CVRE	VALIDATION	VRSQ	VRE	VCE
1901-1940	458	0.796	0.776	1941-1980	0.544	0.555	0.531
1941-1980	363	0.724	0.694	1901-1940	0.688	0.679	0.665
FULL MISSOURI RIVER BASIN – COMMON 95% 2-TAILED SCREENED CHRONOLOGIES							
CALIBRATION	NSER	CRSQ	CVRE	VALIDATION	VRSQ	VRE	VCE
1901-1940	183	0.758	0.736	1941-1980	0.697	0.688	0.671
1941-1980	183	0.668	0.632	1901-1940	0.766	0.760	0.750

Tree-Ring Network Used for reconstruction of HEMO Streamflow

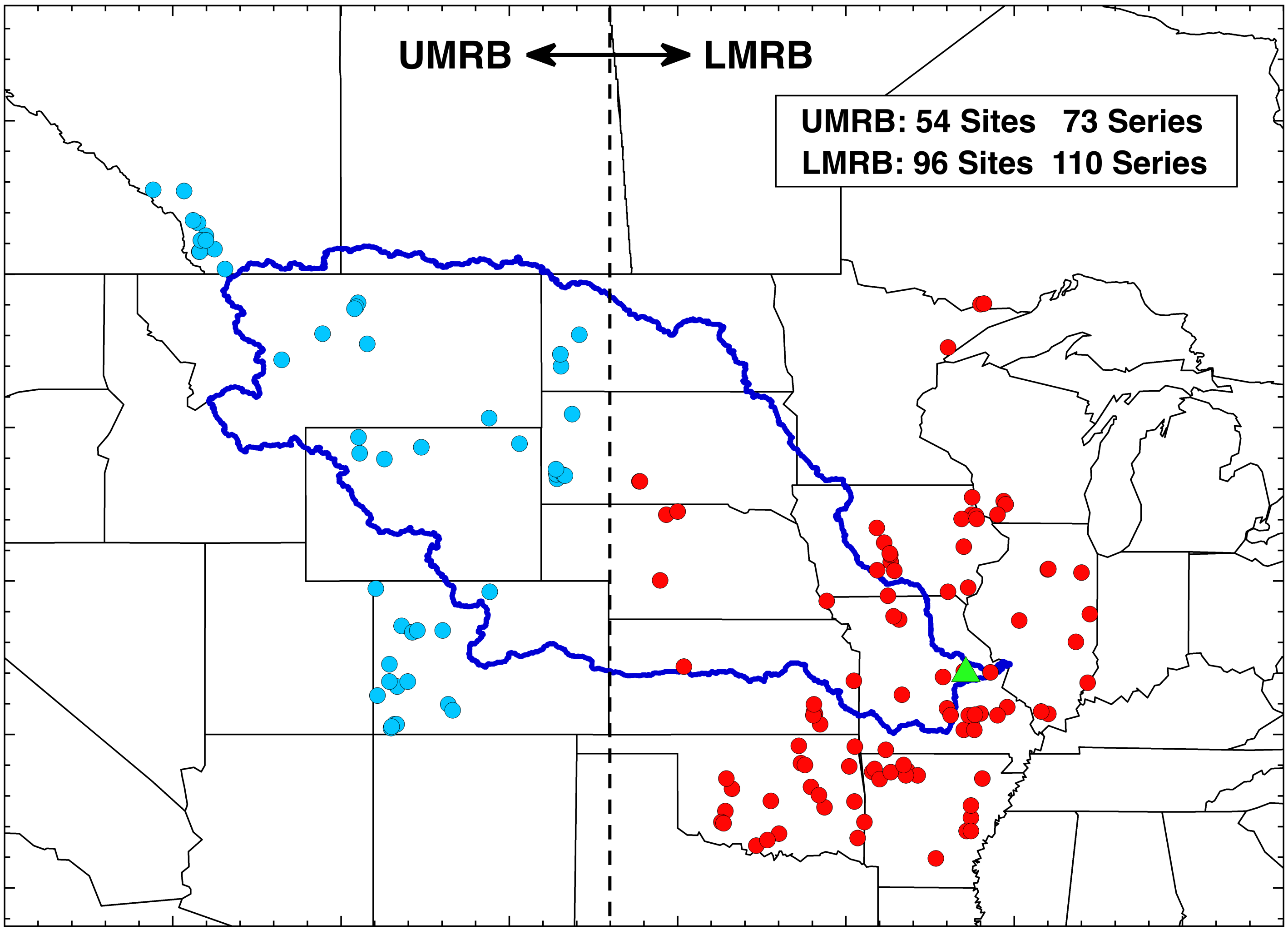

Figure S4. The final tree-ring network (183 chronologies) used to reconstruct water year streamflow at HEMO. The selection was based on the results shown in Table S1 that retained chronologies based on successful calibration in two equal-length, non-overlapping time periods.

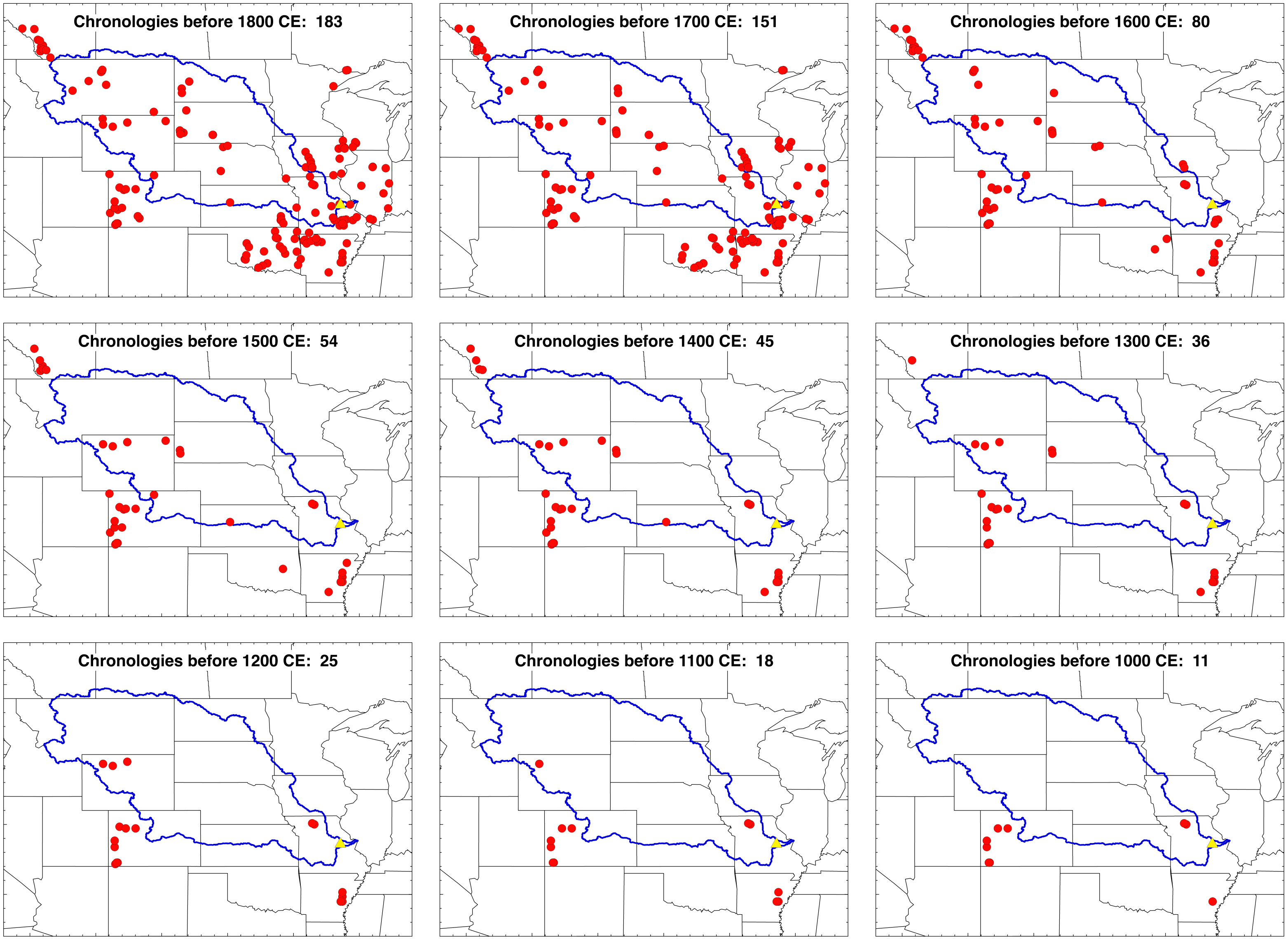

Figure S5. The declining number and distribution of tree-ring chronologies from 1800 CE back to 1000 CE. Before 1400 CE the number and distribution of chronologies for reconstruction at HEMO is increasingly inadequate.

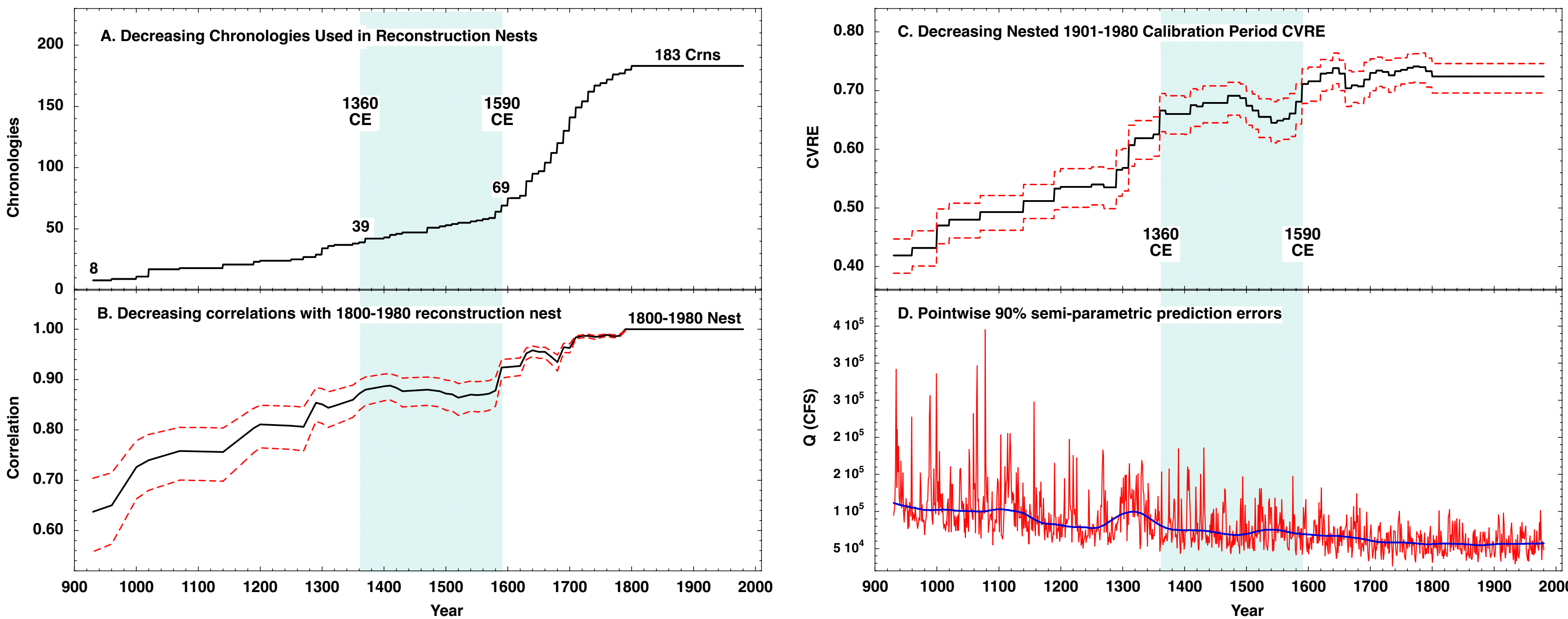

Figure S6. Evaluating HEMO nested reconstruction uncertainty. How far back in time can the reconstruction be trusted? Probably as far back as 1360 CE based on what is shown in S6b (reasonably stable correlation >0.85 from 1590 to 1360 with the best replicated 1800-1980 reconstruction nest) and S6c (reasonably stable leave-one-out CVRE >0.65) even as the number of tree-ring chronologies declines from 69 to 39. Before 1360 both measures of reconstruction stability systematically decline.

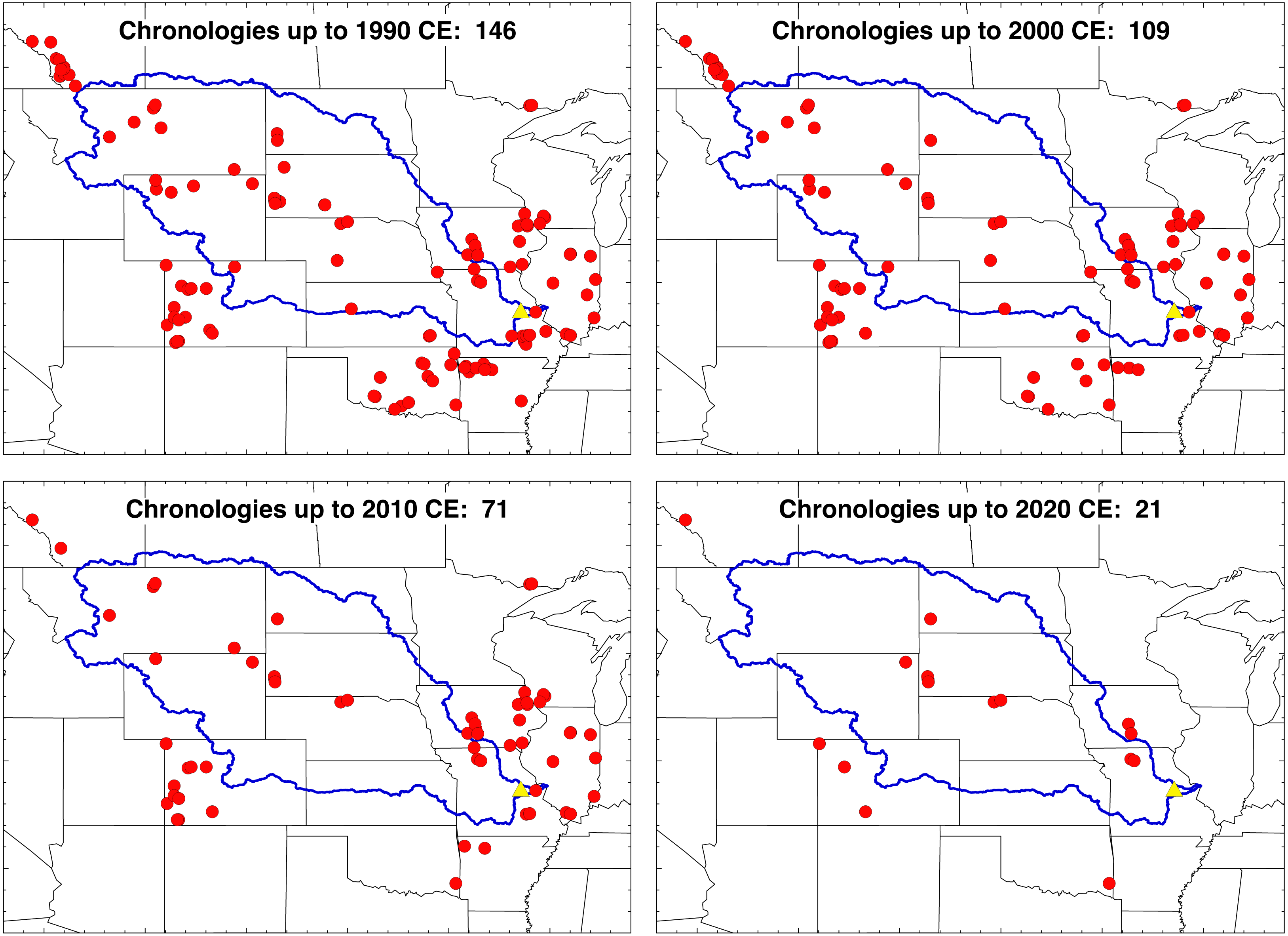

Figure S7. Tree-ring networks used to sequentially extend the HEMO reconstruction forward by 10-year intervals from 1990 to 2020. The 2020 extension is clearly the weakest with respect to number available.

Extended Old HEMO Reconstruction Out To 2020

CALIBRATION	CRNS	CRSQ	CVRE
1901 - 1980	183	0.747	0.737
1901 - 1990	146	0.746	0.736
1901 - 2000	109	0.760	0.750
1901 - 2010	71	0.723	0.711
1901 - 2020	21	0.688	0.675

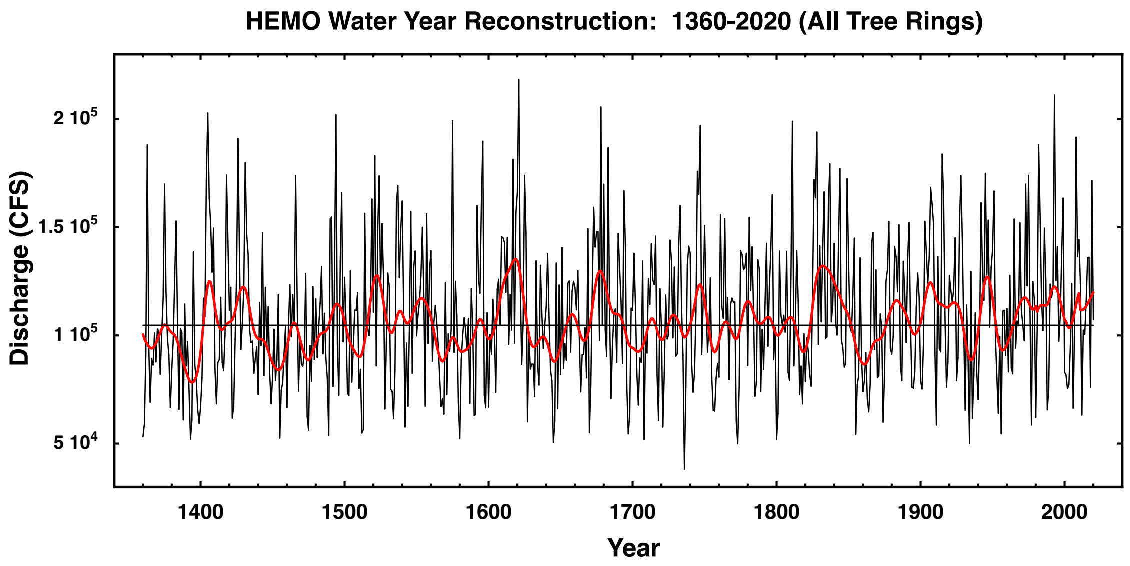

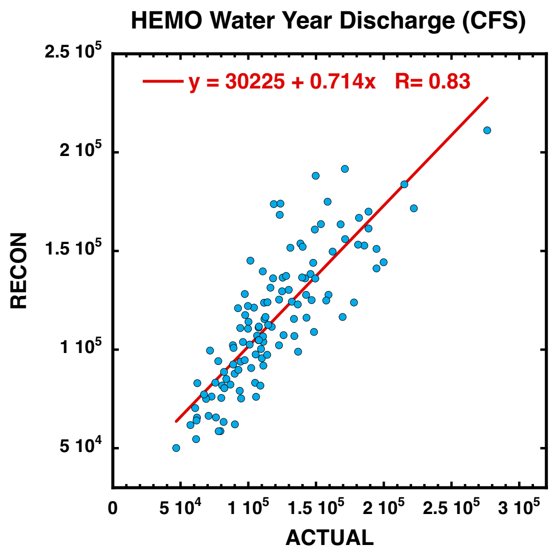

For HEMO based on **PCREG** I estimate uncertainties based on a combination of classical regression **Prediction Intervals** coupled with the **Maximum Entropy Bootstrap**

ELSEVIER

Available online at www.sciencedirect.com

ScienceDirect

Computational Statistics & Data Analysis 51 (2007) 3115–3122

COMPUTATIONAL STATISTICS & DATA ANALYSIS

www.elsevier.com/locate/csda

Prediction intervals for regression models

David J. Olive*

Department of Mathematics, Southern Illinois University, Mailcode 4408, Carbondale, IL 62901-4408, USA

Received 19 June 2005; received in revised form 4 February 2006; accepted 5 February 2006

Available online 28 February 2006

Abstract

This paper presents simple large sample prediction intervals for a future response Y_f given a vector $\boldsymbol{x}_f$ of predictors when the regression model has the form $Y_i = m(\boldsymbol{x}_i) + e_i$ where m is a function of $\boldsymbol{x}_i$ and the errors e_i are iid. Intervals with correct asymptotic coverage and shortest asymptotic length can be made by applying the shorth estimator to the residuals. Since residuals underestimate the errors, finite sample correction factors are needed.

As an application, three prediction intervals are given for the least squares multiple linear regression model. The asymptotic coverage and length of these intervals and the classical estimator are derived. The new intervals are useful since the distribution of the errors does not need to be known, and simulations suggest that the large sample theory often provides good approximations for moderate sample sizes.

ELSEVIER

Available online at www.sciencedirect.com

ScienceDirect

Journal of Asian Economics 17 (2006) 955–978

JOURNAL OF ASIAN ECONOMICS

Maximum entropy ensembles for time series inference in economics☆

Hrishikesh D. Vinod *

Department of Economics, Institute of Ethics and Economic Policy, Fordham University, Bronx, NY 10458, USA

Accepted 6 September 2006

Abstract

This paper uses three examples of potential interest to Asian economists to support a new tool for statistical inference with time series data. In traditional theory, an ensemble Ω represents the 'population' behind the observed time series. Vinod [Vinod, H. D., 2004. Ranking mutual funds using unconventional utility theory and stochastic dominance, Journal of Empirical Finance, 11(3) 2004, 353–377] proposed new maximum entropy (ME) bootstrap to construct J (=999, say) elements of Ω for inference using a seven-step algorithm designed to satisfy the ergodic theorem. The algorithm's practical appeal to applied econometricians is that it avoids all structural change and unit root type testing involving complicated asymptotics and all shape-destroying transformations like de-trending or differencing to achieve stationarity. This paper simplifies and speeds up the algorithm, extends it to panel data, discusses underlying assumptions and formal properties including proving that it satisfies Doob's theorem. We show that the constructed ensemble elements retain the basic shape and dependence structure of autocorrelation function (acf) and partial autocorrelation function (pacf) of the original time series.

MEBoot uncertainty estimation coupled with regression prediction intervals was introduced in:

Contents lists available at SciVerse ScienceDirect

Journal of Hydrology

journal homepage: www.elsevier.com/locate/jhydrol

Five centuries of Upper Indus River flow from tree rings

Edward R. Cook [a,*], Jonathan G. Palmer [b,c], Moinuddin Ahmed [d], Connie A. Woodhouse [e], Pavla Fenwick [c], Muhammad Usama Zafar [d], Muhammad Wahab [d], Nasrullah Khan [d]

[a] *Tree Ring Laboratory, Lamont-Doherty Earth Observatory, Columbia University, Route 9W, Palisades, NY 10964, USA*
[b] *Climate Change Research Centre (CCRC), School of Biological, Earth and Environmental Sciences, The University of New South Wales, Sydney 2052, NSW, Australia*
[c] *Gondwana Tree-ring Laboratory, P.O. Box 14, Little River, Canterbury 7546, New Zealand*
[d] *Botany Department, Federal Urdu University of Arts Science and Technology, Gulshan-e Iqbal, Karachi, Sind 75300, Pakistan*
[e] *School Geography and Development, University of Arizona, P.O. Box 210076, Tucson, AZ 85721, USA*

ARTICLE INFO

Article history:
Received 29 October 2012
Received in revised form 1 February 2013
Accepted 2 February 2013
Available online 13 February 2013
This manuscript was handled by Konstantine P. Georgakakos, Editor-in-Chief

Keywords:
Dendroclimatology
Upper Indus Basin discharge
Streamflow reconstruction from tree rings
Semi-parametric prediction intervals
Discharge regime shifts

SUMMARY

Water wars are a prospect in coming years as nations struggle with the effects of climate change, growing water demand, and declining resources. The Indus River supplies water to the world's largest contiguous irrigation system generating 90% of the food production in Pakistan as well as 13 gigawatts of hydroelectricity. Because any gap between water supply and demand has major and far-reaching ramifications, an understanding of natural flow variability is vital – especially when only 47 years of instrumental record is available. A network of tree-ring sites from the Upper Indus Basin (UIB) was used to reconstruct river discharge levels covering the period AD 1452–2008. Novel methods tree-ring detrending based on the 'signal free' method and estimation of reconstruction uncertainty based on the 'maximum entropy bootstrap' are used. This 557-year record displays strong inter-decadal fluctuations that could not have been deduced from the short gauged record. Recent discharge levels are high but not statistically unprecedented and are likely to be associated with increased meltwater from unusually heavy prior winter snowfall. A period of prolonged below-average discharge is indicated during AD 1572–1683. This unprecedented low-flow period may have been a time of persistently below-average winter snowfall and provides a warning for future water resource planning. Our reconstruction thus helps fill the hydrological information vacuum for modeling the Hindu Kush–Karakoram–Himalayan region and is useful for planning future development of UIB water resources in an effort to close Pakistan's "water gap". Finally, the river discharge reconstruction provides the basis for comparing past, present, and future hydrologic changes, which will be crucial for detection and attribution of hydroclimate change in the Upper Indus Basin.

Shown to be comparable to **Bayesian Regression** credible intervals in:

Research

Six Centuries of Upper Indus Basin Streamflow Variability and Its Climatic Drivers

Mukund Palat Rao[1,2], Edward R. Cook[1], Benjamin I. Cook[3,4], Jonathan G. Palmer[5], Maria Uriarte[6], Naresh Devineni[7,8], Upmanu Lall[8,9], Rosanne D. D'Arrigo[1], Connie A. Woodhouse[10], Moinuddin Ahmed[11], Muhammad Usama Zafar[11], Nasrullah Khan[12], Adam Khan[11], and Muhammad Wahab[13]

[1]Tree Ring Laboratory, Lamont-Doherty Earth Observatory, Columbia University, Palisades, NY, USA, [2]Department of Earth and Environmental Science, Columbia University, New York, NY, USA, [3]NASA Goddard Institute for Space Studies, New York, NY, USA, [4]Ocean and Climate Physics, Lamont-Doherty Earth Observatory, Columbia University, Palisades, NY, USA, [5]ARC Centre of Excellence in Australian Biodiversity and Heritage, School of Biological, Earth and Environmental Sciences, University of New South Wales, Sydney, New South Wales, Australia, [6]Ecology, Evolution, and Environmental Biology, Columbia University, New York, NY, USA, [7]Department of Civil Engineering, The City College of New York, New York, NY, USA, [8]Columbia Water Center, Columbia University, New York, NY, USA, [9]Department of Earth and Environmental Engineering, Columbia University, New York, NY, USA, [10]School of Geography and Development, University of Arizona, Tucson, AZ, USA, [11]Dr. Moinuddin Ahmed Laboratory of Dendrochronology and Plant Ecology, Botany Department, Federal Urdu University of Arts Science and Technology, Karachi, Pakistan, [12]Laboratory of Plant Ecology, Department of Botany, University of Malakand, Chakdara, Pakistan, [13]Botany Department, Women University Swabi, Swabi, Pakistan

Abstract Our understanding of the full range of natural variability in streamflow, including how modern flow compares to the past, is poorly understood for the Upper Indus Basin because of short instrumental gauge records. To help address this challenge, we use Hierarchical Bayesian Regression with partial pooling to develop six centuries long (1394–2008 CE) streamflow reconstructions at three Upper Indus Basin gauges (Doyian, Gilgit, and Kachora), concurrently demonstrating that Hierarchical Bayesian Regression can be used to reconstruct short records with interspersed missing data. At one gauge (Partab Bridge), with a longer instrumental record (47 years), we develop reconstructions using both Bayesian regression and the more conventionally used principal components regression. The reconstructions produced by principal components regression and Bayesian regression at Partab Bridge are nearly identical and yield comparable reconstruction skill statistics, highlighting that the resulting tree ring reconstruction of streamflow is not dependent on the choice of statistical method. Reconstructions at all four reconstructions indicate that flow levels in the 1990s were higher than mean flow for the past six centuries. While streamflow appears most sensitive to accumulated winter (January–March) precipitation and summer (May–September) temperature, with warm summers contributing to high flow through increased melt of snow and glaciers, shifts in winter precipitation and summer temperatures cannot explain the anomalously high flow during the 1990s. Regardless, the sensitivity of streamflow to summer temperatures suggests that projected warming may increase streamflow in coming decades, though long-term water risk will additionally depend on changes in snowfall and glacial mass balance.

PPR can also easily estimate reconstruction uncertainties in two ways: classical parametric prediction intervals and semi-parametric intervals based on applying the *maximum entropy bootstrap* to the data. In either case, the form of the prediction intervals is the same (see Olive, 2007):

$$\hat{Y}_f \pm t_{n-p,1-\alpha/2}\sqrt{MSE}\sqrt{(1+h_f)} \tag{1}$$

where Y_f is the regression estimate, t is the $1-\alpha/2$ t-statistic with $n-p$ degrees of freedom, MSE is the mean square error of the fitted calibration model, and h_f is the "leverage" from the hat-matrix of predictors for each year calculated as:

$$h_f = x_f^T(X^TX)^{-1}x_f \tag{2}$$

where $\boldsymbol{X}$ is the design matrix of predictors used for calibration and x_f is the vector of values used for prediction in year f. The primary difference from Eq. (1) implemented here is that the fixed t-statistic (assume 90% 2-tailed limits) for scaling the uncertainties are replaced by the variable 5th and 95th quantiles (90% quantile limits) from a suite of pseudo-reconstructions produced after applying ME-Boot to both the predictor and predictand data prior to regression.

1000 HEMO Maximum Entropy Bootstrap Pseudo-Reconstructions

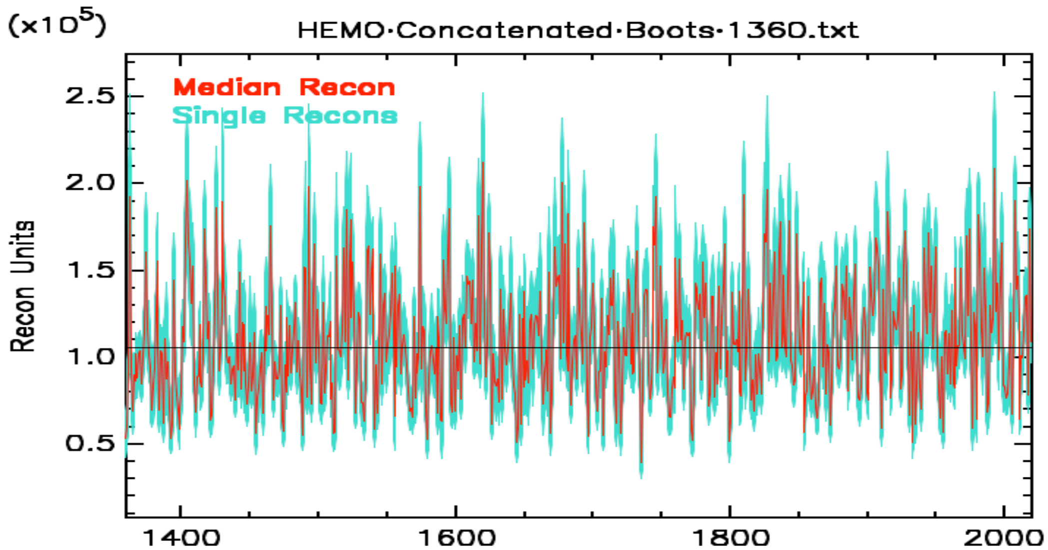

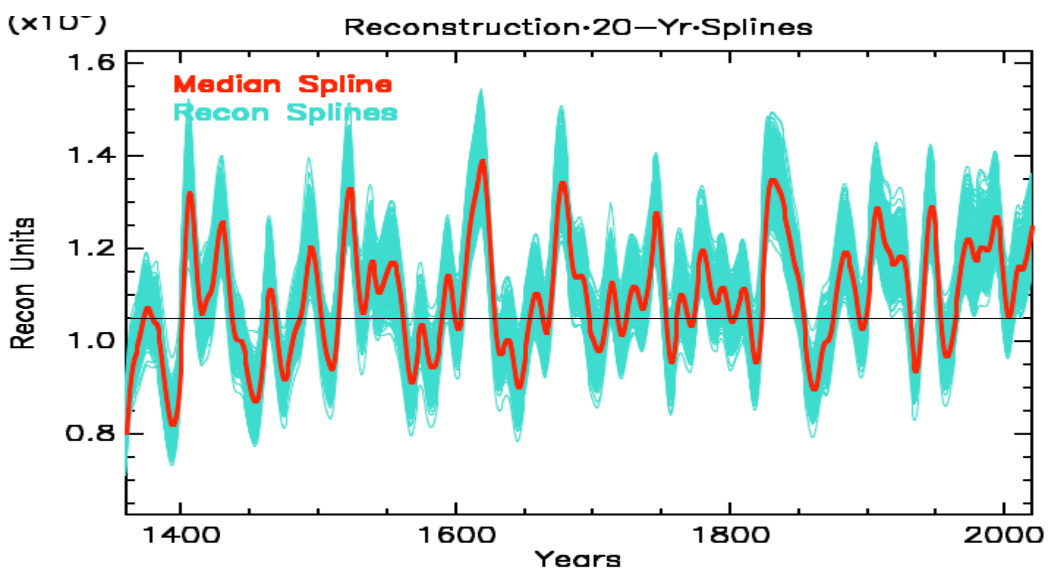

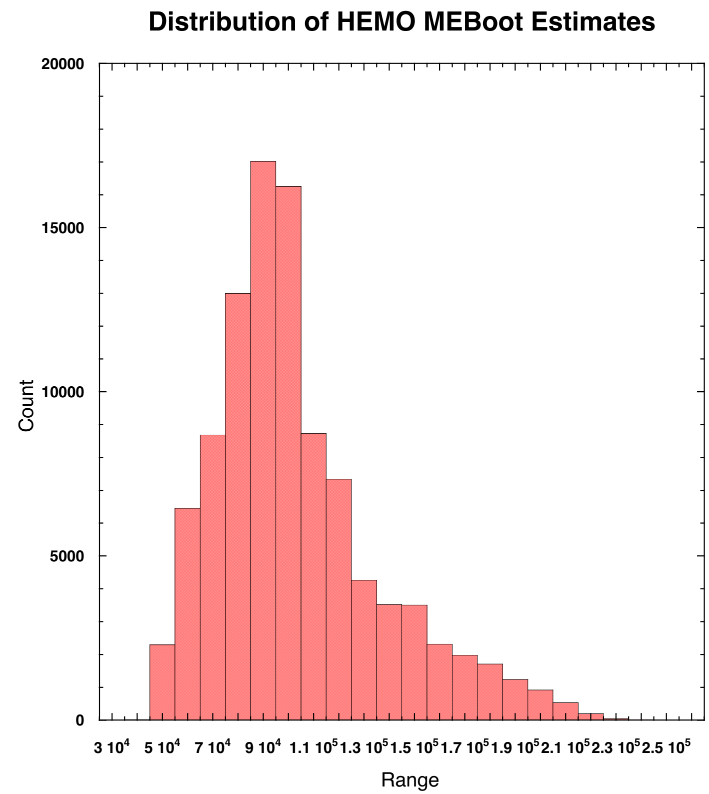

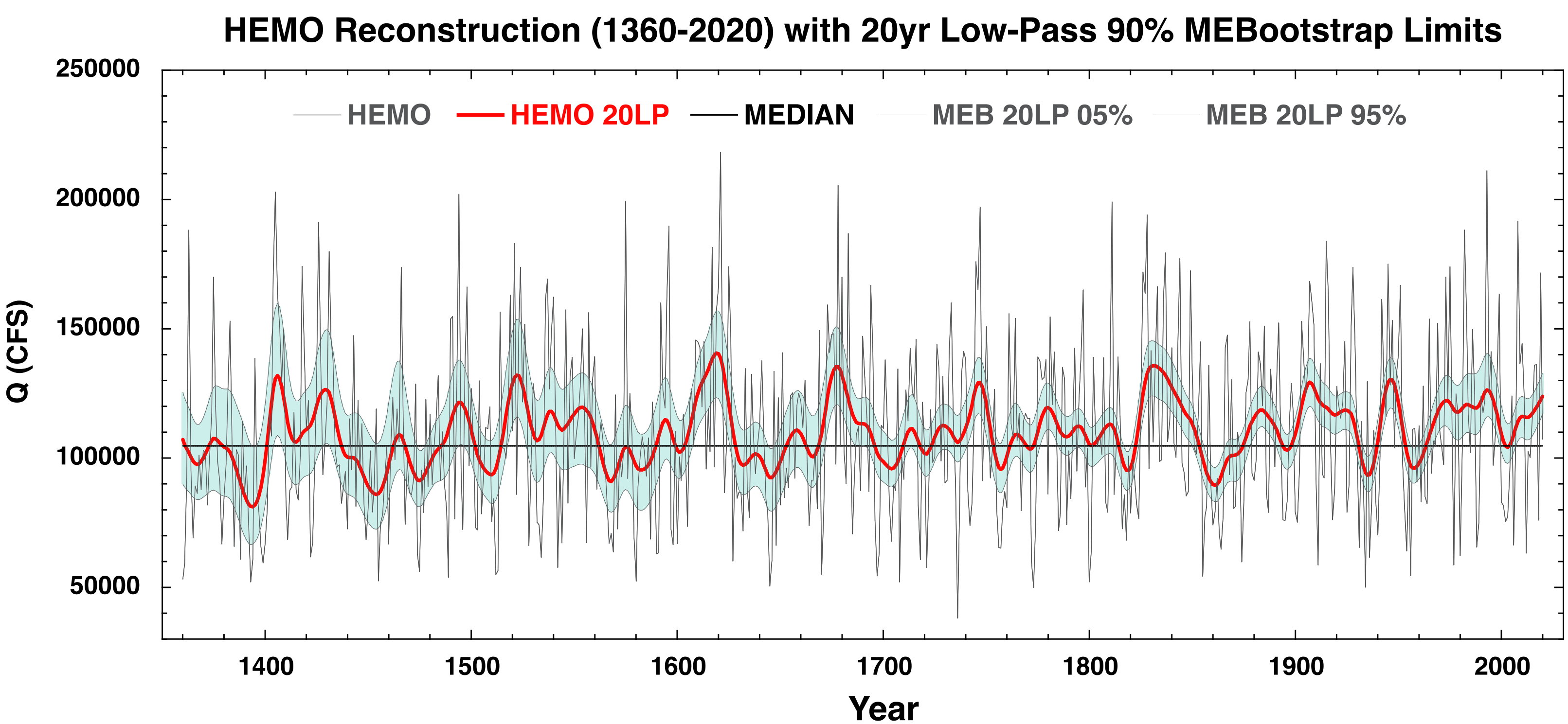
HEMO Reconstruction (1360-2020) with 20yr Low-Pass 90% MEBootstrap Limits
HEMO
HEMO 20LP
MEDIAN
MEB 20LP 05%
MEB 20LP 95%
250000
200000
150000
100000
50000
Q (CFS)
1400
1500
1600
1700
1800
1900
2000
Year

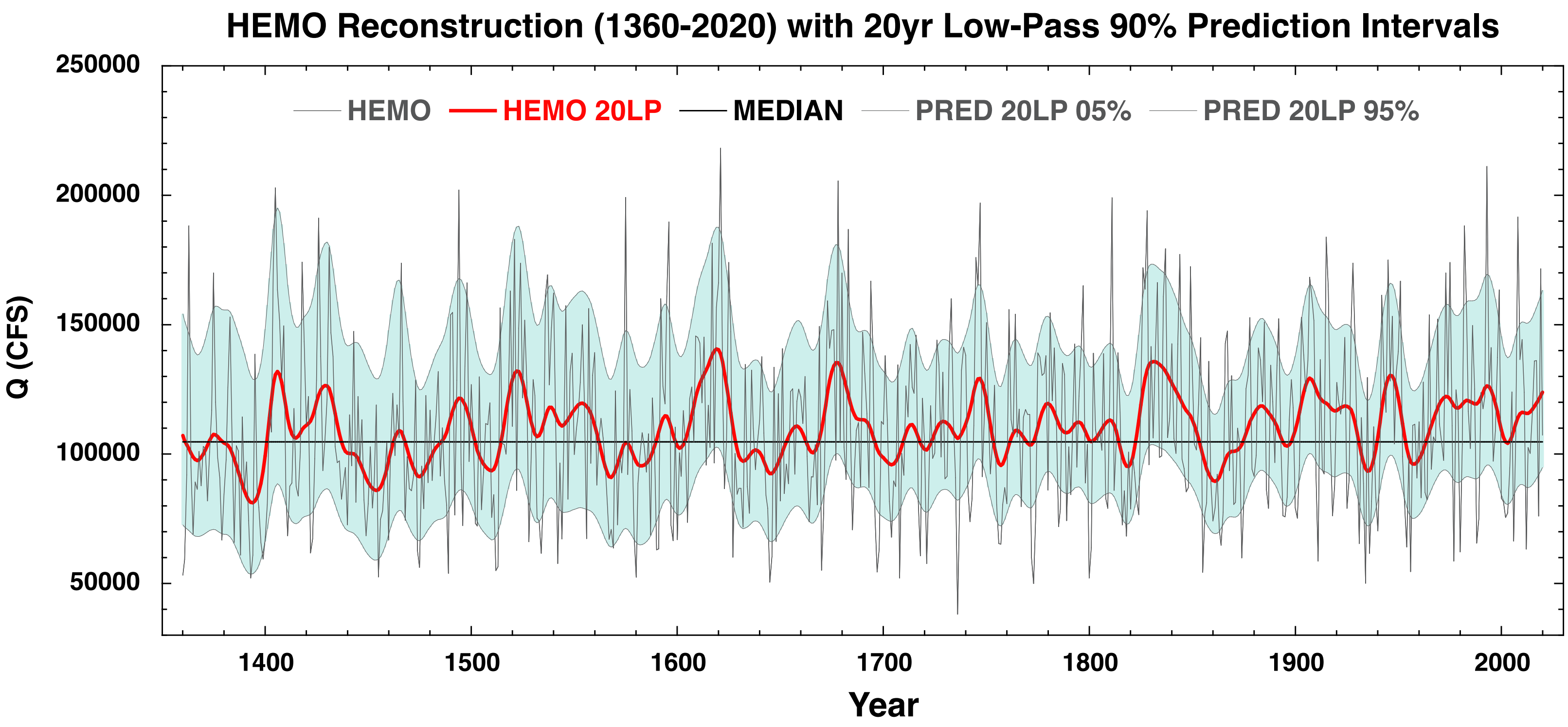
HEMO Reconstruction (1360-2020) with 20yr Low-Pass 90% Prediction Intervals
HEMO
HEMO 20LP
MEDIAN
PRED 20LP 05%
PRED 20LP 95%
250000
200000
150000
100000
50000
Q (CFS)
1400
1500
1600
1700
1800
1900
2000
Year